www.rericjournal.ait.ac.th

The PMSG based Wind Energy Conversion System with CUK Converter and CHB MLI with a Single DC Input

T. Porselvi[*1] and Ranganath Muthu[+]

Abstract – *Wind power is intermittent and hence the electrical output from the wind energy conversion system varies. Therefore, it is necessary to make the output voltage of the wind energy system constant so that it can be connected to the grid. This paper presents a permanent magnet synchronous generator (PMSG) based wind energy conversion system with CUK converter in closed loop and a new topology of cascaded H-bridge multilevel inverter. The paper presents the design of the CUK converter to step-up or step-down the DC voltage of the diode rectifier fed from the wind energy conversion system. The design of a voltage controller to maintain the DC-link voltage constant inspite of the changes in the wind generator voltage due to the changes in the wind speed is also presented in this paper. The DC-link is connected to a new topology of cascaded H-Bridge multilevel inverter. The proposed topology eliminates the requirement of separate DC sources, and requires a single DC source, irrespective of the number of levels and the number of phases. The selective harmonic elimination (SHE) technique is used to produce the switching pulses for the multilevel inverter. The entire system is simulated in the MATLAB/Simulink for varying wind speeds. The simulated waveforms of the wind speed, the PMSG voltage, the DC-link voltage and the multilevel inverter voltage are shown for varying wind speeds. The simulation results show that the output voltage of the system is maintained constant even though the wind speed is varying.*

Keywords – Cascaded H- Bridge Inverter, CUK converter, permanent magnet synchronous generator, wind turbine, voltage controller.

1. INTRODUCTION

Efforts are being made to generate the electrical power from renewable energy sources due to the increased demand of the electric power. Wind energy is the most popular among the various renewable energies. Generation of the wind electrical energy has increased due to the development of power electronic converters. In addition, the wind energy has many advantages like being easily available, safe, cheap and pollution free. The use of the wind energy in electrical power system has introduced new challenges in the transmission and the distribution systems. The wind electric energy can be obtained by a system that consists of a wind turbine, a generator, power electronic converters and a control system [1]. Power electronic converters are more important in achieving high efficiency and good performance in the wind energy conversion systems (WECS). Initially, the WECS were of fixed speed type with the squirrel cage induction generators being used. In the fixed speed type, the speed of the wind turbine is constant irrespective of the wind speed and is determined by the frequency of the grid. The fixed speed turbines are designed to achieve the maximum output only at one speed [2]. Today, variable speed wind energy conversion systems are more popular with the permanent magnet synchronous generator (PMSG) and the doubly fed induction generator (DFIG) as they have many advantages over fixed speed wind turbines like increased energy capture, operation at the maximum power point, higher efficiency, and improved power quality [3]. Variable speed system with the PMSG is more attractive compared to the DFIG because of the various advantages like being directly connected to the wind turbine without any gear box arrangement, not requiring any excitation and hence not requiring slip rings, being less costly and requiring less maintenance [4]. The PMSG can be connected to the grid directly through a full-power converter. The use of the power converter between the generator and the grid provides decoupling between them. The use of a full-scale power converter allows full controllability; it is possible to run the generator at any desired speed and have a fixed frequency on the grid side [5]. PMSGs are classified as radial flux PMSGs, axial flux PMSGs and transverse flux PMSGs based on the direction of the flux lines. They are also classified as surface inset PMSGs, surface mounted PMSGs and interior PMSGs based on the location of the permanent magnets on the rotor [6]. The surface mounted PMSG is the most efficient of the PMSGs and hence used in most of the PMSG based wind energy systems.

The output voltage of a wind generator is a variable one as the wind speed is not constant. The voltage of the wind generator increases with the increase in wind speeds and decreases with decrease in wind speed. In this paper, for overcoming the above, a CUK converter is used to step-up the voltage at lower wind speeds and step-down the voltage at higher wind speeds. However, it is necessary to maintain the output voltage of the CUK converter at a constant value for making it suitable for any particular application.

*Electrical and Electronics Engineering, Sri SaiRam Engineering College, Chennai, India.

[+]Electrical and Electronics Engineering, SSN College of Engineering, Chennai, India

[1]Corresponding author:
E-mail address: tporselvi@yahoo.com.

The arrangement of the paper is as follows: section 2 deals with the system description, which includes the wind turbine model, the PMSG model, the diode rectifier, the CUK converter, the conventional CHB multilevel inverter and the CHB inverter with a single DC source and the PI controller design. Section 3 explains the simulation and the results and the conclusion is brought out in section 4.

2. SYSTEM DESCRIPTION

Figure 1 show the block diagram of the entire system, which consists of a wind turbine coupled to a permanent magnet synchronous generator. The generator converts the mechanical energy of the wind turbine into electrical energy. The electrical output of the generator, which is AC, is connected to a three-phase diode bridge rectifier. The diode rectifier converts the AC voltage of the PMSG into DC voltage. The output of the diode rectifier is connected to a CUK converter. The CUK converter steps-up or steps-down the voltage for decreasing or increasing wind speeds respectively. The DC output of the CUK converter is converted to AC of the desired frequency using the new cascaded H-bridge multilevel inverter. This inverter requires a single DC source, unlike the conventional cascaded H-Bridge multilevel inverter that requires many DC sources. A PI controller maintains the output voltage of the CUK converter at the desired reference value.

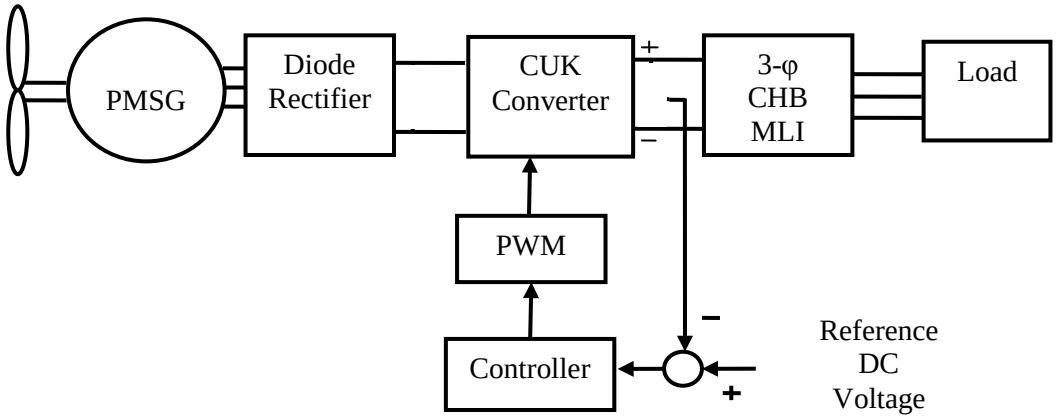

Fig. 1 Block diagram of the proposed wind energy conversion system.

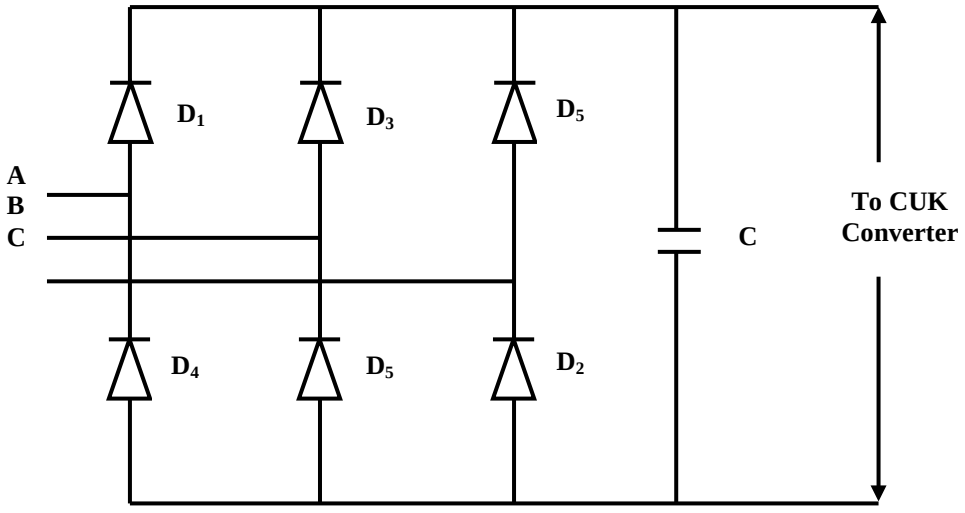

Fig. 2 Three phase diode bridge rectifier.

2.1 Wind Turbine Model

The rotor of the wind turbine has to extract the maximum power from the wind. Equation (1) gives the power obtained from the wind,

$$P_W = \frac{1}{2} c_p \rho A v^3 \quad (1)$$

where, ρ is the air density, $A = \pi R^2$ is the swept area of the rotor in m^2, R is the radius of the rotor in m,

c_p is the power co-efficient and v is the wind speed in m/s.

Equation (2) gives the value of c_p, which is a function of the tip speed ratio λ and the pitch angle γ,

$$c_p = c_1[c_2\frac{1}{\beta} - c_3\gamma - c_4\gamma^x - c_5]e^{-c_6\frac{1}{\beta}} \quad (2)$$

where, $$\lambda = \frac{\omega R}{v} \quad (3)$$

$$\frac{1}{\beta} = \frac{1}{\lambda + 0.08\gamma} - \frac{0.035}{1+\gamma^3} \quad (4)$$

ω is the rotor speed in rad/s, the coefficients c_1 to c_6 and x are dependent on the wind turbine type and dimensions. Equation (5) gives the aerodynamic torque in Nm.

$$\tau_w = \frac{P_w}{\omega} \quad (5)$$

The mechanical torque of the generator and the aerodynamic torque are equal as gearbox is not used [7].

2.2 PMSG Model

The PMSG is modeled in the synchronous rotating d-q reference frame with the d-axis aligned with the permanent magnet axis. Equations (6) and (7) give the voltage equations in the d-q reference frame,

$$v_d = R_s i_d - \omega_e \psi_q + \frac{d\psi_d}{dt} \quad (6)$$

$$v_q = R_s i_q + \omega_e \psi_d + \frac{d\psi_q}{dt} \quad (7)$$

where, v_d and v_q are the d axis and the q axis voltages respectively, i_d and i_q are respectively the d axis and the q axis currents, ω_e is the electrical angular velocity of the rotor in rad/s, R_s is the per phase resistance of the stator winding, ψ_d and ψ_q are the d axis and the q axis flux linkages respectively [7]. Equations (8) and (9) give the d axis and the q axis flux linkages,

$$\psi_d = L_d i_d + \psi_{pm} \quad (8)$$

$$\psi_q = L_q i_q \quad (9)$$

where, L_d is the d axis per phase stator inductance, L_q is the q axis per phase stator inductance and ψ_{pm} is the permanent magnet flux linkage. Equations (10) and (11) give the voltage equations after substituting for ψ_d and ψ_q.

$$v_d = R_s i_d - \omega_e L_q i_q + \frac{d(L_d i_d + \psi_{pm})}{dt} \quad (10)$$

$$v_q = R_s i_q + \omega_e (L_d i_d + \psi_{pm}) + \frac{d(L_q i_q)}{dt} \quad (11)$$

Since ψ_{pm} is constant, its derivative is zero. Hence, Equation (10) becomes the Equation (12).

$$v_d = R_s i_d - \omega_e L_q i_q + \frac{d(L_d i_d)}{dt} \quad (12)$$

Equation (13) gives the electromagnetic torque of the PMSG,

$$T_e = \frac{3p}{2}(\psi_d i_q - \psi_q i_d) \quad (13)$$

where, p is the number of pairs of poles. Equations (14) and (15) respectively give the active power and the reactive power [7].

$$P = \frac{3}{2}(v_d i_d + v_q i_q) \quad (14)$$

$$Q = \frac{3}{2}(v_q i_d - v_d i_q) \quad (15)$$

2.3 Diode Rectifier

The diode rectifier converts the three-phase voltage of the PMSG into DC voltage. Figure 2 shows the circuit of three-phase diode bridge rectifier.

Equation (16) gives the average output voltage of the rectifier,

$$V_{oavg} = \frac{3V_{ml}}{\pi} \quad (16)$$

where, V_{ml} is the peak value of the line voltage of the PMSG.

2.4. CUK Converter and Its Design

The output of the diode bridge rectifier is connected to the CUK converter. The CUK converter is used to step-up the DC link voltage at lower wind speeds and to step-down the DC link voltage at higher wind speeds. It has the advantage of having a continuous input current, which is not the case for a buck - boost converter. Figure 3 shows the circuit of CUK converter.

(a) Analysis of the CUK converter

The analysis is done for the continuous conduction mode of operation. There are two modes of operation of the CUK converter. Mode I operation of the converter occurs when the switch is ON, and the mode II operation occurs when the switch is OFF.

Mode I

In mode I, the switch is in the ON condition, the diode is in the OFF condition. Figure 4 shows the circuit for mode I operation. Equations (17-22) give the equations governing the mode I operation. Equation (17) gives the voltage across the inductor L_1 during the ON period,

$$L_1\frac{di_{L1}}{dt} = V_i \quad (17)$$

where, V_i is the input DC voltage. If ΔI_1 is the ripple current of the inductor L_1 current during T_{ON}, then the equation (17) becomes equation (18).

$$L_1\frac{\Delta I_1}{T_{ON}} = V_i \quad (18)$$

$$\Delta I_1 = \frac{V_i T_{ON}}{L_1} \quad (19)$$

Equation (20) gives the voltage across the inductor L_2 during the ON period,

$$L_2 \frac{di_{L2}}{dt} = V_{c1} + V_{DC} \quad (20)$$

where, V_{c1} is the average voltage of C_1. V_{DC} is the average voltage of capacitor C_2 or the average output voltage of the CUK converter. If ΔI_2 is the ripple current of the inductor L_2 during T_{ON}, then the Equation (20) becomes Equation (21).

$$L_2 \frac{\Delta I_2}{T_{ON}} = V_{c1} + V_{DC} \quad (21)$$

$$\Delta I_2 = \frac{(V_{c1} + V_{DC}) T_{ON}}{L_2} \quad (22)$$

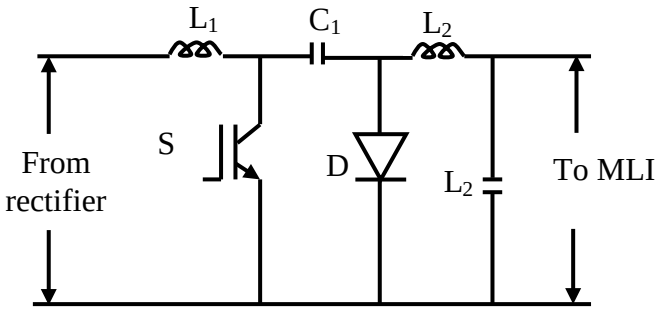

Fig. 3 CUK Converter.

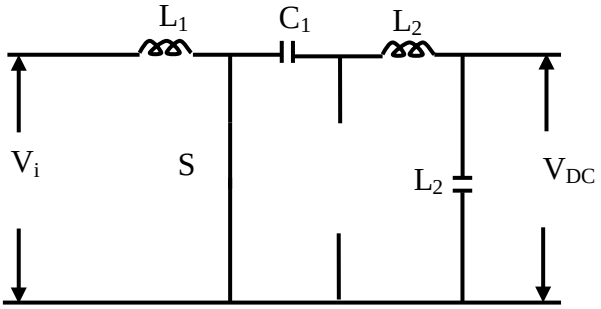

Fig. 4 Circuit for mode I with 'S' ON and 'D' OFF

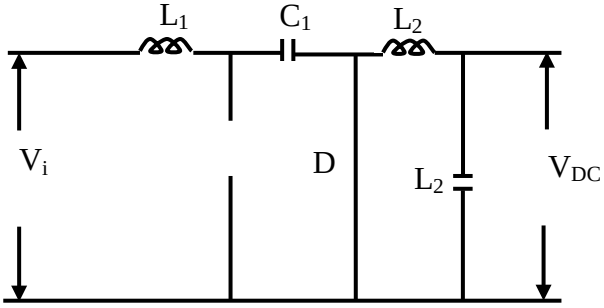

Fig. 5 Circuit for mode II with 'S' OFF and 'D' ON

Mode II

In mode II, the switch is in the OFF condition and the diode is in the ON condition. Figure 5 gives the circuit for the mode II.

Equations (23-28) give the equations governing the mode II operation. Equation (23) gives the voltage across the inductor L_1 during the OFF period.

$$L_1 \frac{di_{L1}}{dt} = V_i - V_{c1} \quad (23)$$

The change in current of inductor L_1 in mode II is $-\Delta I_1$ and hence Equation (23) becomes Equation (24).

$$-L_1 \frac{\Delta I_1}{T_{OFF}} = V_i - V_{c1} \quad (24)$$

$$\Delta I_1 = \frac{-(V_i - V_{c1})T_{OFF}}{L_1} \quad (25)$$

Equation (26) gives the voltage across the inductor L_2 during the OFF period.

$$L_2 \frac{di_{L_2}}{dt} = V_{DC} \quad (26)$$

The change in the current in inductor L_2 in mode II is $-\Delta I_2$, and hence equation (26) becomes equation (27).

$$-L_2 \frac{\Delta I_2}{T_{OFF}} = V_{DC} \quad (27)$$

$$\Delta I_2 = \frac{-(V_{DC})T_{OFF}}{L_2} \quad (28)$$

Equating equations (19) & (25), and (22) & (28) and substituting T_{ON}=kT and T_{OFF}=(1-k)T, the average voltage of capacitor C_1 is given by equations (29) and (30),

$$V_{c1} = \frac{V_i}{1-k} \quad (29)$$

$$V_{c1} = -\frac{V_{DC}}{k} \quad (30)$$

where, k is the duty ratio of the switch 'S'. Equating Equations (29) and (30), the average output voltage of the converter is given by Equation (31).

$$V_{DC} = -\frac{kV_i}{1-k} \quad (31)$$

Equations (32)-(35) give the design equations of the CUK converter for the continuous conduction mode [8],

$$L_1 = \frac{kV_i}{f\Delta I_1} \quad (32)$$

$$L_2 = \frac{kV_i}{f\Delta I_2} \quad (33)$$

$$C_1 = \frac{(1-k)I_i}{f\Delta V_{C1}} \quad (34)$$

$$C_2 = \frac{kV_i}{8L_2 f^2 \Delta V_{C2}} \quad (35)$$

where, I_i is the input current, f is the switching frequency. ΔV_{c1} and ΔV_{c2} are the ripple voltages of the capacitors C_1 and C_2 respectively. Using the above equations the inductor and capacitor values are found to be L_1=0.3 mH, C_1=0.15 μF, L_2=0.5 mH and C_2=0.16 mF.

2.5 Multilevel Inverter with a Single DC Source

The output of the CUK converter is connected to a multilevel inverter. Multilevel inverters (MLIs) are used in renewable energy applications for boosting the low source voltage to a higher voltage for transmitting power to the loads or to the grid. They have higher efficiency because of lower switching losses and lesser total harmonic distortion (THD), lower electromagnetic interference effects, reduced voltage stresses across the switches, higher voltage capability as compared to conventional inverters [9]-[11]. Unlike the neutral point clamped multilevel inverter and the flying capacitor multilevel inverter, the cascaded H-bridge (CHB) multilevel inverter does not require any clamping diodes or capacitors and hence is suitable for high power applications [12]-[14].

The conventional CHB multilevel inverter uses identical H-bridges in cascade. For an m-level inverter, there are ($\frac{m-1}{2}$) identical H-bridges. A separate DC source is required for each individual H-bridge [15]. Figure 6 shows the single leg of the conventional five-level CHB multilevel inverter. The inverter uses two separate DC sources. Each DC source has a single-phase H-bridge inverter.

(a) Cascaded H-Bridge (CHB) multilevel inverter with a single DC source

The paper proposes a new topology of the CHB multilevel inverter. The proposed topology incorporates the advantages of the conventional CHB inverter and eliminates the disadvantage of using separate DC sources. The new topology can be easily used in the renewable energy conversion system as it requires a single DC input, unlike the conventional inverter. If the conventional CHB inverter is to be used in the system, we need to use capacitors, which should be charged in advance. For an m-level inverter, ($\frac{m-1}{2}$-1) capacitors per phase are required. This increases the cost and the problems due to charging and discharging also occur. The proposed CHB inverter uses only one DC source irrespective of the number of levels and the number of phases of the inverter and ($\frac{m-1}{2}$) low frequency (fundamental frequency) transformers. Hence, the cost is much reduced and is best suited for the wind energy conversion system where only one DC output is available from the DC-link.

Figure 7 shows the circuit of one leg of the proposed five-level CHB multi level inverter. It uses a single DC source and ($\frac{m-1}{2}$) number of transformers for an m-level inverter.

Figure 8 shows the circuit of the proposed three-phase five level inverter. The circuit requires a single DC source and two three-phase transformers. The secondary windings of the two transformers are connected in series and the series connected secondary windings are connected in star fashion, which is connected to the three phase star connected load.

Table 1 shows the comparison of the components used in the conventional and the proposed three-phase five-level CHB inverters.

(b) Modeling of five-level inverter

The modeling of inverter is carried out by assuming the binary factors of each leg to be zero or one [16]. Equations (36)-(39) give the binary factors of the four legs,

$$H_{11} = \begin{cases} 0, S_1 = \text{off}, S_3 = \text{on} \\ 1, S_1 = \text{on}, S_3 = \text{off} \end{cases} \quad (36)$$

$$H_{21} = \begin{cases} 0, S_2 = \text{off}, S_4 = \text{on} \\ 1, S_2 = \text{on}, S_4 = \text{off} \end{cases} \quad (37)$$

$$H_{12} = \begin{cases} 0, S_1' = \text{off}, S_3' = \text{on} \\ 1, S_1' = \text{on}, S_3' = \text{off} \end{cases} \quad (38)$$

$$H_{22} = \begin{cases} 0, S_2' = \text{off}, S_4' = \text{on} \\ 1, S_2' = \text{on}, S_4' = \text{off} \end{cases} \quad (39)$$

where, H_{11} and H_{21} are the binary states of the first and second leg of the first bridge respectively, H_{12} and H_{22} are the binary states of the first and second leg of the second bridge respectively.

Table 2 shows the possible switching states of the inverter and the corresponding output voltage V_o for one leg.

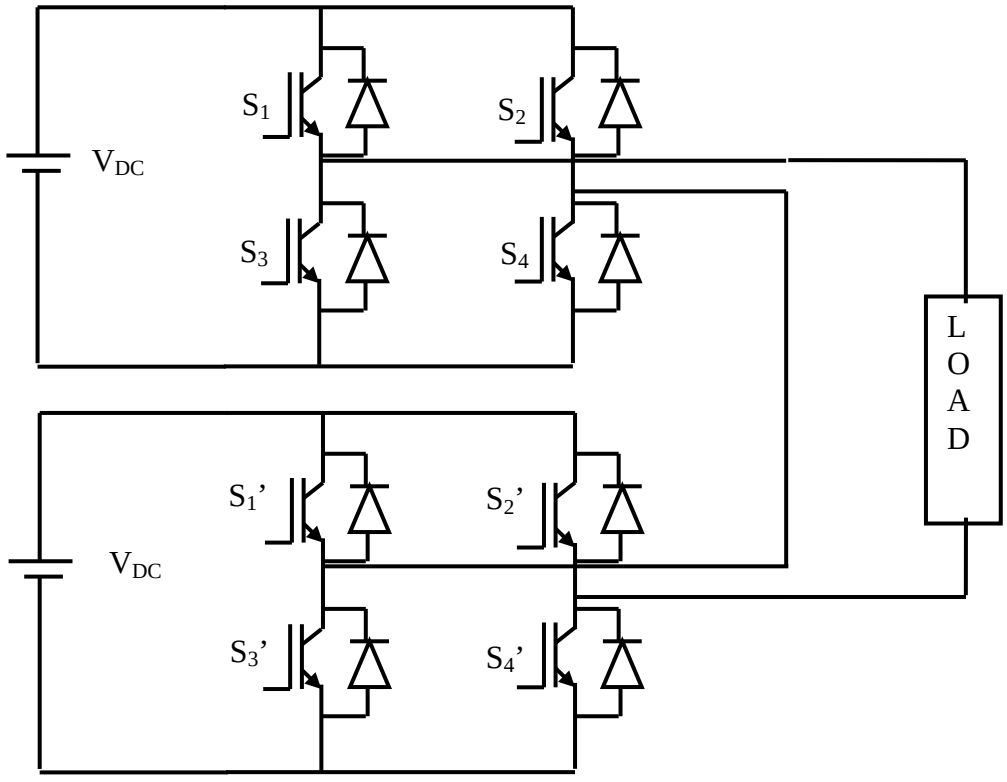

Fig. 6. Single leg of the conventional five-level CHB multilevel inverter

Table 1. Comparison of the conventional and the proposed three-phase five-level CHB MLI.

Type of CHB MLI	Number of IGBT/Diode pairs required	No. of DC sources required	No. of transformers required
Conventional CHB MLI	24	6	0
Proposed CHB MLI	24	1	3

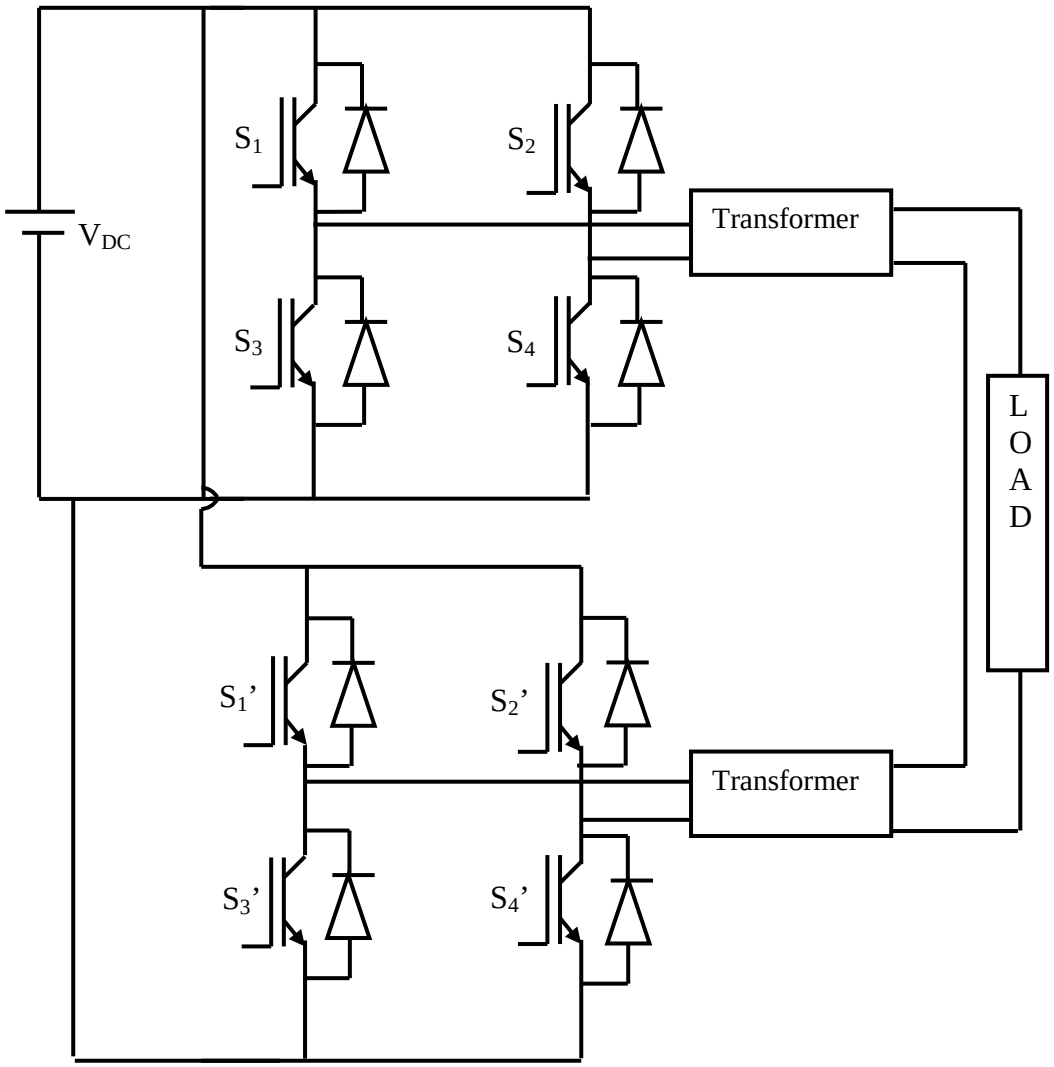

Fig. 7. Single leg of the proposed five-level CHB inverter with a single DC source.

Table 2. Switching states of one leg of the five-level inverter

H_{11}	H_{21}	H_{12}	H_{22}	V_o
0	0	0	0	0
0	0	0	1	$-V_{DC}$
0	0	1	0	V_{DC}
0	0	1	1	0
0	1	0	0	$-V_{DC}$
0	1	0	1	$-2V_{DC}$
0	1	1	0	0
0	1	1	1	$-V_{DC}$
1	0	0	0	V_{DC}
1	0	0	1	0
1	0	1	0	$2V_{DC}$
1	0	1	1	V_{DC}
1	1	0	0	0
1	1	0	1	$-V_{DC}$
1	1	1	0	V_{DC}
1	1	1	1	0

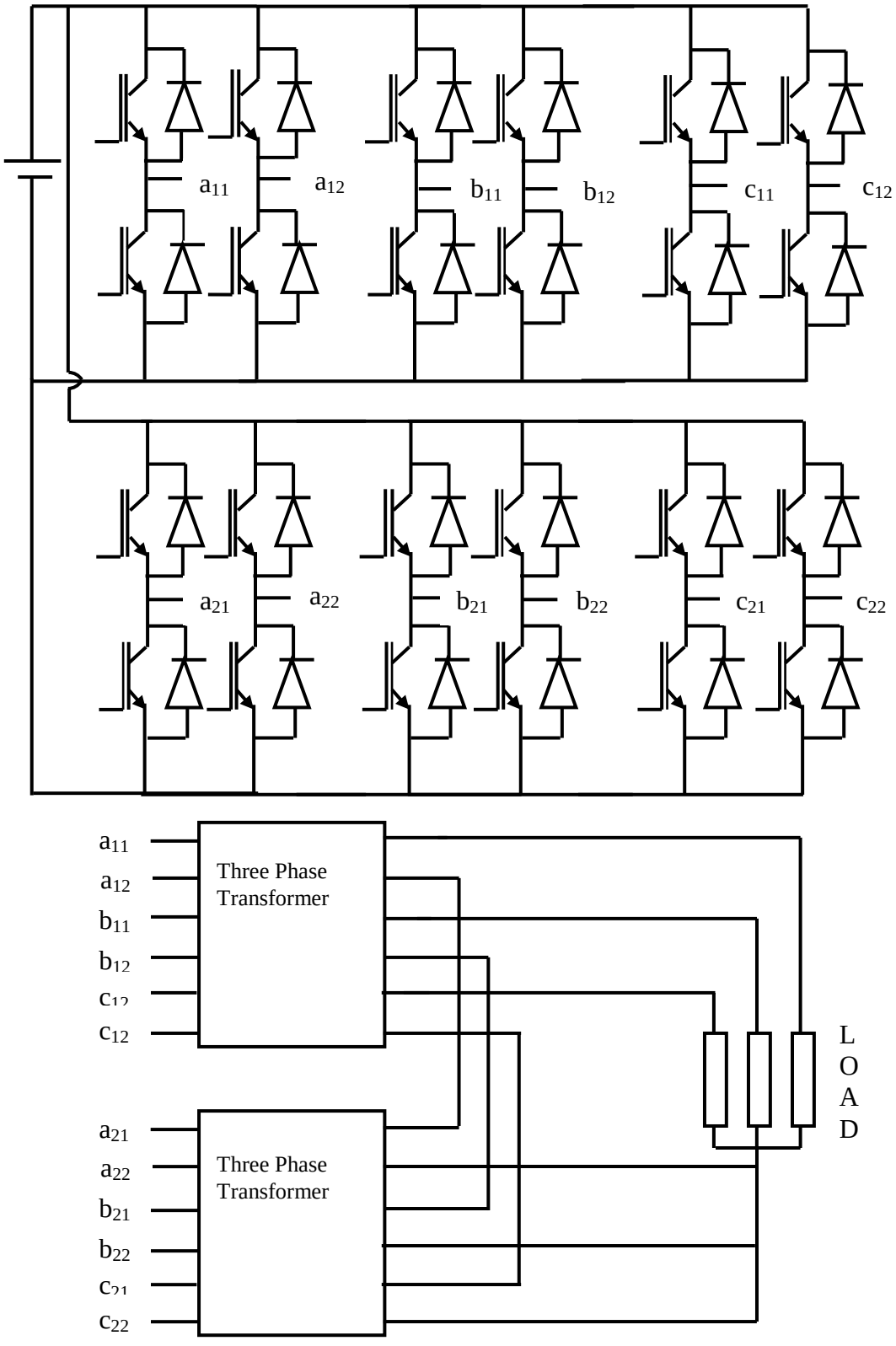

Fig. 8. Circuit of proposed three-phase five-level CHB inverter with a single DC source.

(c) Selective Harmonic Elimination

There are many switching techniques available for the multilevel inverters, the most popular and simple technique is the multi-carrier PWM technique. However, this technique requires high frequency carrier signals and hence the switching losses increase. Therefore, the switching technique at the fundamental frequency is desired. Selective harmonic elimination at the fundamental frequency is the best PWM technique, which produces the desired fundamental value with the elimination of the dominant lower harmonics [17]-[19].

The proposed multilevel inverter (MLI) is controlled using the selective harmonic elimination PWM (SHE-PWM) at the fundamental frequency. The

multilevel output voltage is obtained by switching ON and OFF the semiconductor switches in such a manner that the fundamental voltage of desired magnitude is obtained with less harmonic distortion. In this technique, the switching angles are computed by solving the transcendental equations characterizing harmonics [20]. For a five-level inverter, two switching angles are generated by solving the two transcendental equations describing the fundamental and the third harmonic components. These equations are solved using the Newton - Raphson method, which is one of the fastest iterative methods. This method solves the transcendental equations with the initial approximate values [21].

The output voltage waveform of the five-level inverter, which is a staircase waveform, can be expressed using Fourier series as given by equation (40),

$$v_o(\omega t) = \sum_{n=1,3,5}^{\infty} \frac{4V_{DC}}{n\pi}(\cos(n\theta_1) + \cos(n\theta_2))\sin(n\omega t) \quad (40)$$

where, θ_1 and θ_2 are the switching angles of the five-level inverter, and $0< \theta1< \theta2< \pi/2$. From the equation (40), the fundamental voltage is given by equation (41) [22].

$$V_1 = \frac{4V_{DC}}{\pi}(\cos(\theta_1) + \cos(\theta_2)) \quad (41)$$

The maximum value of the fundamental voltage obtainable which is the value of the fundamental voltage when all the switching angles are zero is $V_{m1} = \frac{4sV_{DC}}{\pi}$, and $s = \frac{m-1}{2}$. The modulation index M_I is the ratio of the fundamental voltage to maximum fundamental voltage. $M_I = \frac{V_1}{V_{m1}}$. Two equations can be formed to describe the fundamental and the third harmonic voltages. The third harmonic is eliminated by equating the third harmonic voltage equation to zero. Equations (42) and (43) give the two equations to be solved to get the switching angles [23].

$$\cos(\theta_1) + \cos(\theta_2) = \frac{\pi V_1}{4V_{DC}} \quad (42)$$

$$\cos(3\theta_1) + \cos(3\theta_2) = 0 \quad (43)$$

Solving these equations by Newton -Raphson method, the switching angles are found to be θ_1=0.179 rad and θ_2=0.87 rad for M_I=0.8.

2.6. PI Controller

The proportional plus integral (PI) controller is used as a voltage controller, which maintains the output voltage of the CUK converter at a constant value. PI controllers are widely used because they have only two parameters to be tuned, one being proportional to the error between the reference and the actual output; another being proportional to the integral of the error [24-25].

The controller is tuned using the Ziegler Nichol's method of tuning (second method of tuning). The various steps of this method are as follows

1. The converter is simulated to run with zero integral gain (K_i). The value of proportional gain (K_p) is increased from zero to a critical value K_{pcr} until an oscillation of constant magnitude is obtained.
2. The critical value of the proportional gain K_{pcr} and the period of the sustained oscillation T_{cr} are noted.
3. The PI controller gains are given by the following equations (44)-(46).

$$K_P = 0.45K_{pcr} \quad (44)$$

$$T_i = \frac{T_{cr}}{1.2} \quad (45)$$

$$K_i = \frac{K_P}{T_i} \quad (46)$$

Using the above equations the K_p and K_i values are found to be 0.0005 and 0.003.

3. SIMULATION AND RESULTS

The whole system is simulated in MATLAB/ Simulink software for varying wind speeds. The simulated waveforms of the wind speed, the output voltage of PMSG (phase 'a' voltage), the output voltage of CUK converter, the line voltage of the MLI, and the phase voltage of MLI are shown.

In Figure 9, the wind speed is varied as follows: 6 m/s from 0 s to 2.5 s, 12 m/s from 2.5 s to 5 s and 7 m/s from 5 s onwards.

From Figure 10 it is seen that the output voltage of PMSG for phase 'a' is 150 V until 2.5 s. The output voltage increases to 350 V as the wind speed increases from 6 ms to 12 m/s. The output voltage decreases to around 175 V at 5 s as the wind speed decreases to 7m/s at 5 seconds.

Figure 11 shows the output voltage of the CUK converter and the line voltage of the MLI.It is seen from the Figure 11 that the output voltage of the CUK converter is maintained at 225 V. The CUK converter voltage increases at 2.5 s seconds due to the change in the wind speed and the PMSG voltage. The CUK converter voltage reaches the reference DC voltage of 225 V at 3 seconds due to the PI controller action. In addition, the CUK converter voltage decreases at 5 s due to the decrease in the wind speed and the PMSG voltage, but the voltage again settles to 225 V volts at 5.5 s due to the PI action. Hence, the CUK converter voltage (DC link voltage) is maintained at the constant value at 225 V even though the wind speed and hence the PMSG voltages are changed, due to the PI based voltage controller. It is also evident from the Figure 11 that the line voltage of the MLI is also maintained at a constant value after having changed at 2.5 s and 5 s as it is fed from the CUK converter. Figure 12 shows the line voltage in the expanded scale. Figure 13 shows the switching pulses for the three legs of the multilevel inverter.

Figure 14 shows the phase voltage of MLI and Figure 15 shows the phase voltage in expanded scale. It is evident from Figures 11-15 that the CUK converter voltage, the MLI line voltages and the MLI phase voltages are maintained at the constant value after having changed due to the changes in the wind speed by the PI controller action.

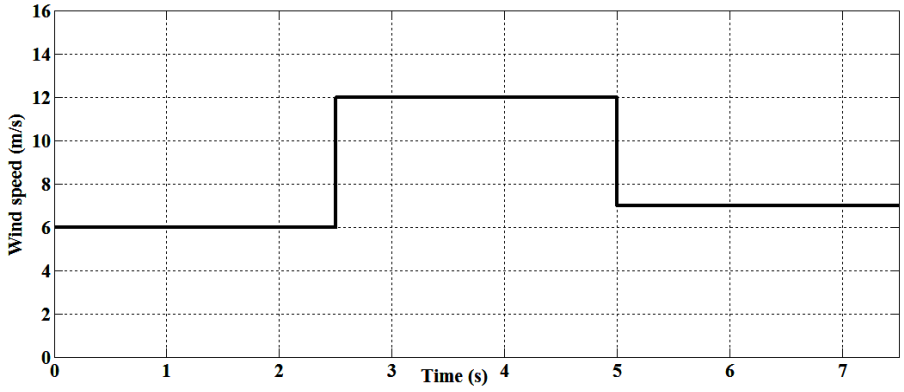

Fig. 9. Wind speed (m/s).

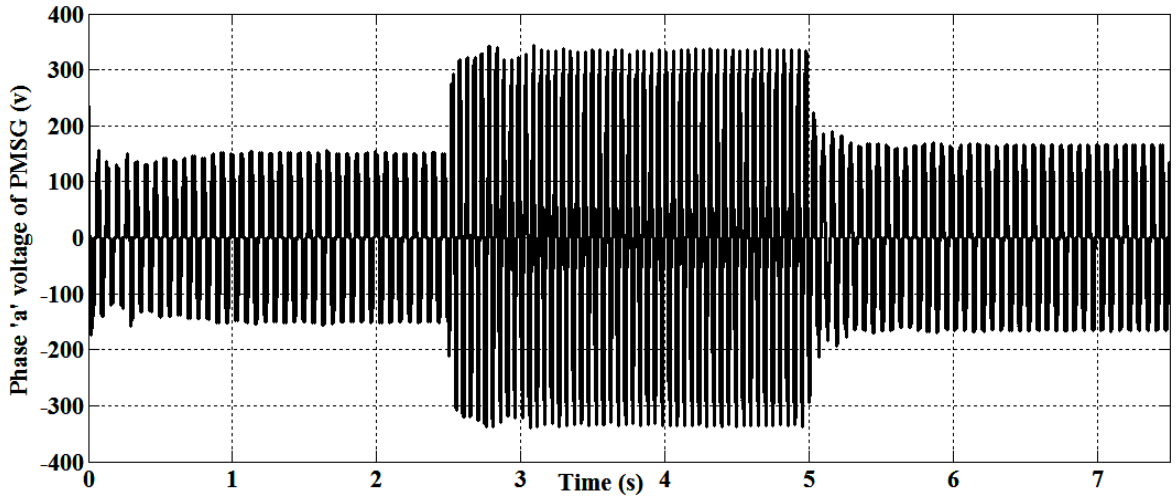

Fig. 10. Output voltage of PMSG (phase 'a' voltage).

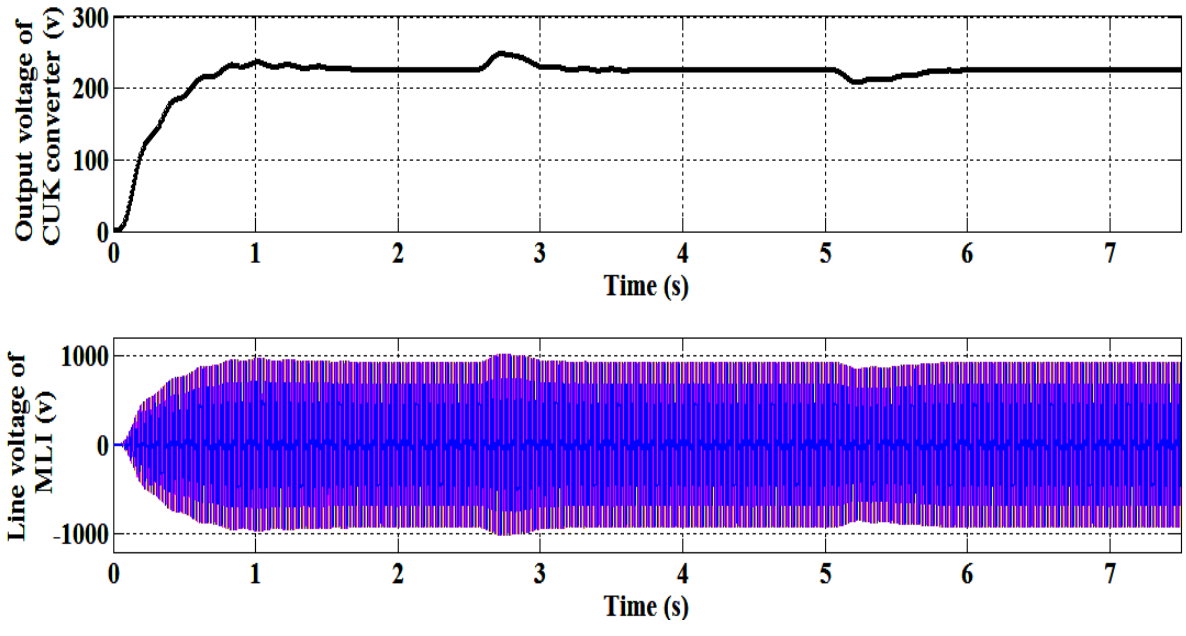

Fig. 11. Output voltage (volts) of CUK converter and line voltage (volts) of MLI.

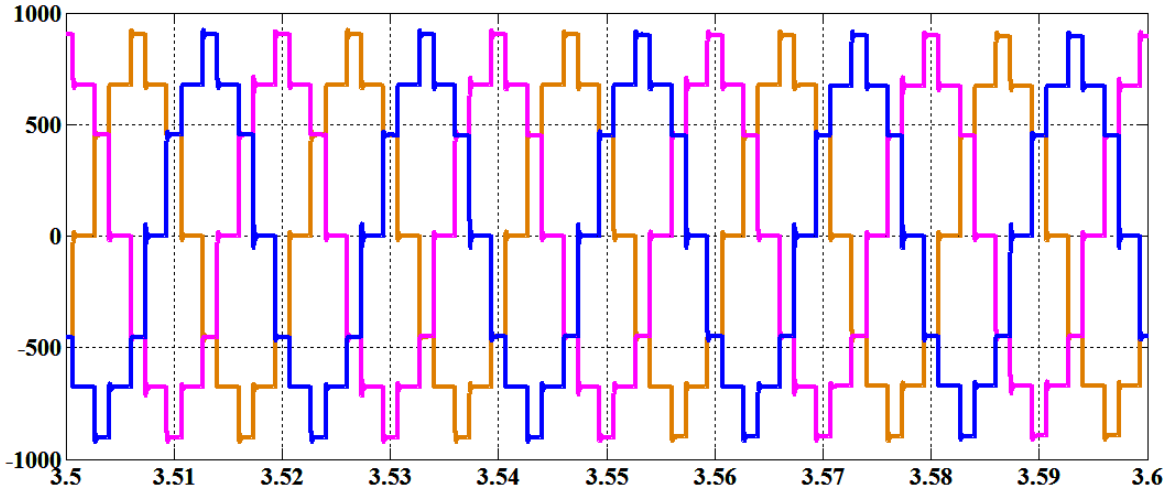

Fig. 12. Line voltage (volts) of MLI in expanded scale.

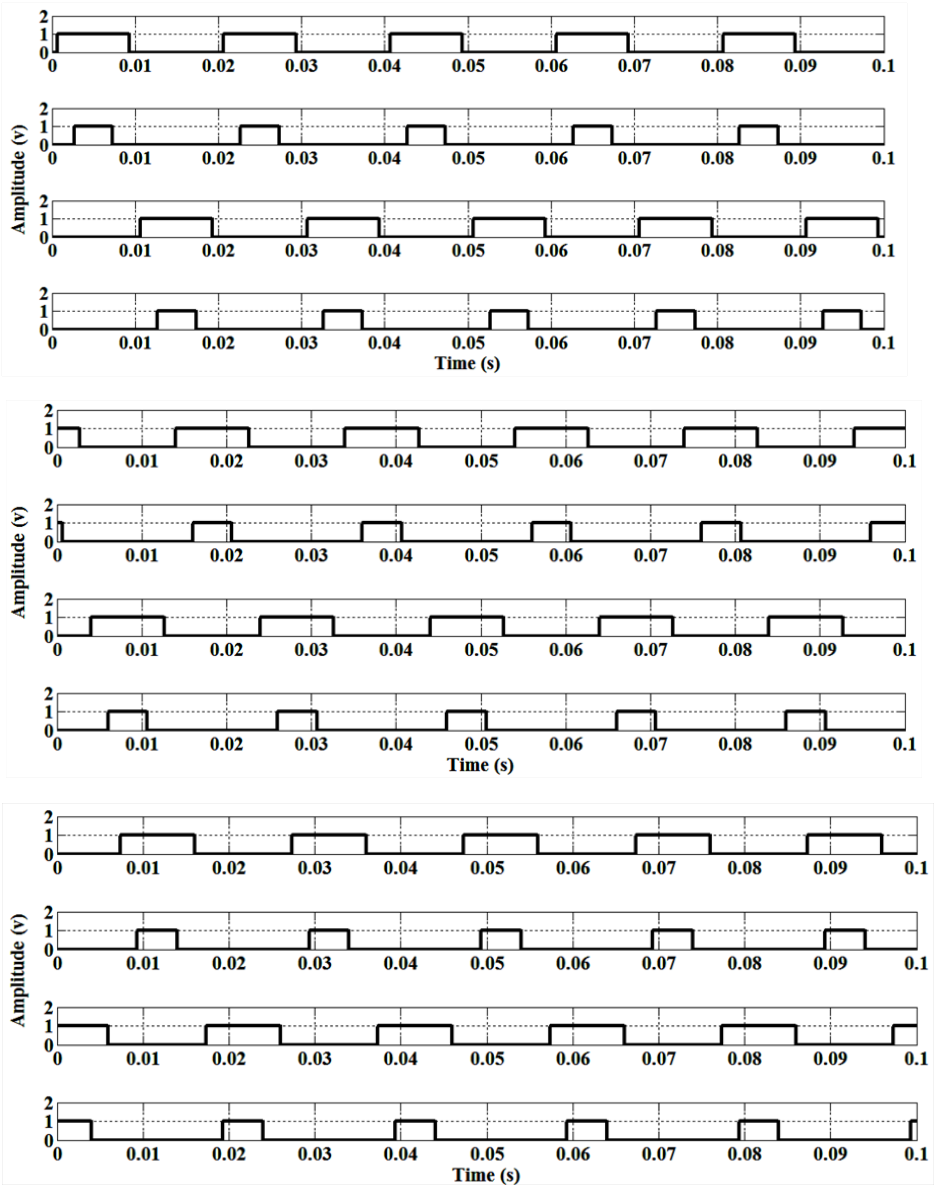

Fig. 13. Switching patterns for the three legs of the three phase MLI.

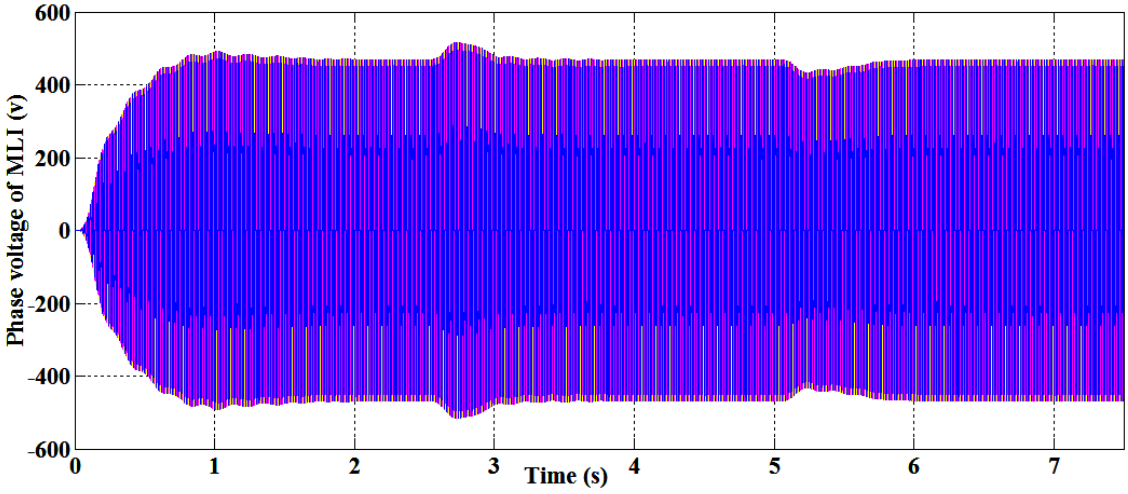

Fig. 14. Phase voltage (volts) of proposed MLI.

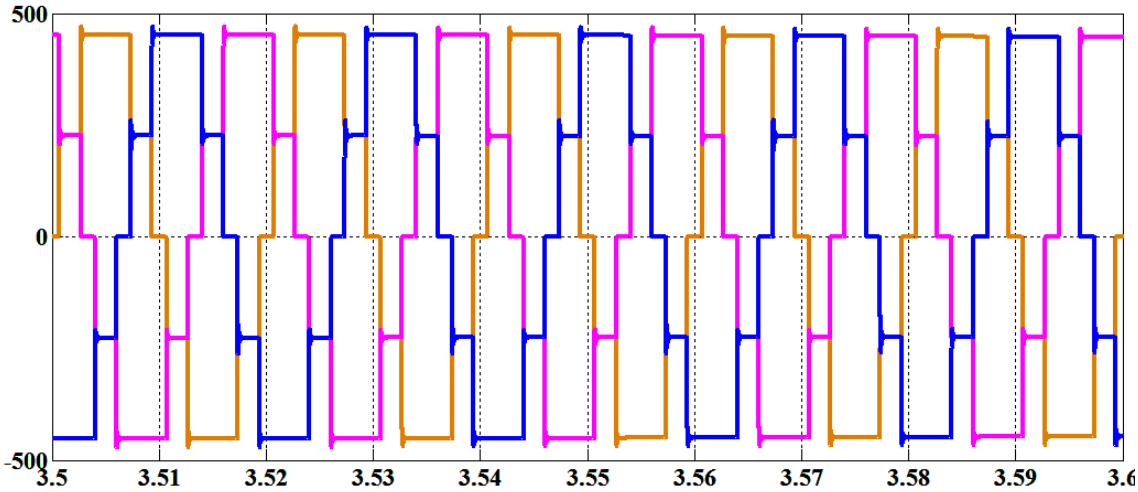

Fig. 15. Phase voltage (volts) of MLI in expanded scale.

4. CONCLUSIONS

A PMSG based wind energy conversion system is proposed. A CUK converter is designed for the wind generator, which steps up or steps down the generator voltage for decreasing or increasing wind speeds. A PI controller is designed to maintain the DC link voltage (i.e. the output voltage of the CUK converter) at the desired value. A new topology of CHB multi level inverter is proposed. The proposed topology includes the advantages of the conventional CHB inverter and eliminates the disadvantage of requiring separate DC sources. The proposed topology requires a single DC source irrespective of number of levels and number of phases and hence the cost is much reduced. The proposed circuit produces the multilevel output voltage in an efficient way with the use of fundamental frequency three-phase transformers. Since the inverter is switched with SHE-PWM technique of fundamental frequency, the switches operate at the fundamental frequency, switching losses and electromagnetic interferences are reduced very much. The output voltage of the multilevel inverter is also maintained at a constant value as the input to the MLI is fed by the CUK converter whose output is regulated by the PI controller. The waveforms of the wind speed, the generator voltage, the DC link voltage and the inverter voltages were shown for both increasing and decreasing wind speeds. It is observed from the waveforms that the designed CUK converter is able to step up the voltage when the wind speed is decreasing and vice versa. It is also noted that the designed PI voltage controller is able to maintain the DC link voltage at the desired value with the increase and decrease of the wind speeds.

NOMENCLATURE

P_w	Power obtained from wind in watts
ρ	Density of air
c_p	Power co-efficient
v	Wind speed in m/s
A	Rotor swept area of the wind turbine
λ	Tip speed ratio
Υ	Pitch angle
ω	Rotor speed in rad/s
τ_w	Aerodynamic torque
v_d	Stator voltage of PMSG in d-axis

v_q	Stator voltage of PMSG in q-axis
i_d	Stator current of PMSG in d- axis
i_q	Stator current of PMSG in q- axis
R_s	Stator per phase resistance
ω_e	Rotor electrical speed in rad/s
ψ_d	d-axis flux linkage
ψ_q	q-axis flux linkage
ψ_{pm}	Permanent magnet flux linkage
L_d	Per phase stator inductance in d-axis
L_q	Per phase stator inductance in q-axis
T_e	Electromagnetic torque of PMSG
P	Active power of PMSG
Q	Reactive power of PMSG
p	Number of pair of poles of PMSG
V_{oavg}	Average output voltage of the diode rectifier
V_{ml}	Line voltage of the PMSG
k	Duty ratio of the CUK converter
L_1, L_2	Inductances of the CUK converter
C_1, C_2	Capacitances of the CUK converter
V_{DC}	Average output voltage of the CUK converter
V_i	Input voltage of CUK converter
ΔI_1	Ripple current of L_1
ΔI_2	Ripple current of L_2
V_{c1}	Average capacitor (C_1) voltage
ΔV_{c1}	Ripple voltage of C_1
ΔV_{c2}	Ripple voltage of C_2
f	Switching frequency of the CUK converter switch
m	Number of levels of the CHB inverter
H_{11}, H_{21}	binary states of the first and second leg of the first bridge of CHB inverter respectively
H_{12} H_{22}	binary states of the first and second leg of the second bridge of CHB inverter respectively
V_o	Output voltage of the CHB inverter for one phase
Θ_1,Θ_2	Switching angles of the CHB inverter
n	Harmonic number of the output voltage of CHB inverter
M_I	Modulation index
V_1	Fundamental voltage
V_{m1}	Maximum fundamental voltage
K_p	Proportional gain of PI controller
K_i	Integral gain of PI controller
K_{pcr}	Critical value of the proportional gain
T_{cr}	Period of the sustained oscillation
T_i	Integral time constant

REFERENCES

[1] Kumar V., Joshi R.R. and Bansal R.C., 2009. Optimal control of Matrix-Converter-Based WECS for Performance Enhancement and Efficiency Optimization. *IEEE Transaction on Energy Conversion* 24(1): 264-273.

[2] Ackermen T., 2005. *Wind Power in Power Systems*, John Wiley and Sons, Ltd.

[3] Müller S., Deicke M. and De Doncker R.W., 2002. Doubly fed induction generator system for wind turbines. *IEEE Ind. Appl. Mag.* 8(3): 26–33.

[4] Haque M.E., Muttaqi K.M. and Negnevitsky M., 2008. Control of a standalone variable speed wind turbine with a permanent magnet synchronous generator. *IEEE Power and Energy Society General Meeting - Conversion and Delivery of Electrical Energy in the 21st Century*, 1-9.

[5] Mehrzad D., Luque J. and Cuenca M.C., *Vector Control of PMSG for Grid Connected Wind Turbine Applications.* Master's thesis, Institute of Energy Technology, Alborg University. Chapter 1, page 1.

[6] Porselvi T. and R. Muthu. 2011. Simulation of Surface Mounted Permanent Magnet Synchronous Generator. In *Proceedings of the 1st International Conference on Electrical Energy Systems ~ICEES 2011~*, India. 3-5 Jan.

[7] Porselvi T. and R. Muthu. 2012. Design of buck-boost converter for wind energy conversion system. *European Journal of Scientific Research*, 83(3): 397-407.

[8] Rashid M.H., 2007. *Power Electronics Circuits, Devices and Applications*, Low Price Edition, Chapter 5- DC-DC Converter, pp 198-104. Academic Press.

[9] Lai J.-H. and F.Z. Peng., 1996. Multilevel converters - a new breed of power converters. *IEEE Transactions on Industry Applications*, 32(3), 509-517.

[10] Peng F.Z., McKeever J.W. and Adams D.J. 1997. Cascaded Multilevel Inverters for Utility Applications. *IECON Proceedings (Industrial Electronics Conference)* 2: 437-442.

[11] Urmila B. and D. Subbarayudu D., 2010. Multilevel inverters: a comparative study of pulse width modulation techniques. *International Journal of Scientific & Engineering Research*, 1(3), 1-5.

[12] Rodríguez J., Lai J.-S. and Peng F.Z., 2002. Multilevel inverters: a survey of topologies, control and applications. *IEEE Transactions on Industrial Electronics* 49(4): 724-738.

[13] Carrara G., Gardella S., Marchesoni M., Salutari R. and Sciutto G., 1992. A new multilevel PWM method: a theoretical analysis. *IEEE Transactions on Power Electronics*, 7(3): 497-505.

[14] Porselvi T. and R. Muthu. 2011. Comparison of cascaded H-Bridge, neutral point clamped and flying capacitor multilevel inverters using multicarrier PWM. In *Proceedings of INDICON 2011-Annual IEEE India Conference*, Hyderabad, India, December 16-18.

[15] Prathiba T. and P. Renuga. 2012. A comparative study of total harmonic distortion in multi level inverter topologies. *Journal of Information Engineering and Applications* 2(3): 26-36.

[16] Galvan J.I.L. *Multilevel Converters: Topologies, Modelling, Space Vector Modulation Techniques and Optimisations.* Doctoral Thesis University of Seville, Electronic Engineering Department, Power Electronics Group. Chapter 2-Multilevel Converter Topologies, 33-36.

[17] Chaisson J.N., Tolbert L.M., Mckenzie K.J. and Du, Z., 2004. A unified approach to solving the harmonic elimination equations in multilevel converters. *IEEE Transactions on Power Electronics* 19(2): 478-490.

[18] Sirisukprasert S., Lai S. and Liu T.H., 2002. Optimum harmonic reduction with a wide range of modulation indexes for multilevel converters. *IEEE Transactions on Industrial Electronics* 49(4): 875-881.

[19] Bouhali O., Berkouk E.M., Saudemont C. and Francois B., 2004. A five level diode clamped inverter with self-stabilization of the DC-link voltage for grid connection of distributed generators. In *Proceeding of IEEE International Symposium on Industrial Electronics: ISIE 2004*, Ajaccio, France, May 3-7.

[20] Peng F.Z., Lai J.-S., McKeever J. and VanCoevering J., 1996. A multilevel voltage-source inverter with separate DC sources for static var generation. *IEEE Transactions on Industry Applications* 32(5): 1130-1138.

[21] Woodford C. and C. Phillips. 1997. *Numerical Methods with Worked Examples.* First edition; London; Chapman and Hall. 45-57.

[22] Kumar J. and B. Das. 2008. Selective harmonic elimination technique for a multilevel inverter. In *Proceeding of Fifteenth National Power Systems Conference (NPSC),* IIT Bombay, December.

[23] Udhaya Shankar C., Thamizharasi J., Thottungal R. and Nithyadevi N., 2012. Harmonic reduction in cascaded multilevel inverter with reduced number of switches with genetic algorithm. *International Journal of Advances in Engineering & Technology*, 3(1): 284-294.

[24] Basilio J.C. and S.R. Matos. 2002. Design of PI and PID controllers with transient performance specification. *IEEE Transactions on Education* 45(4): 364-370.

[25] Shyama M. and P. Swaminathan. 2012. Digital linear and nonlinear controllers for buck converter. *International Journal of Soft Computing and Engineering (IJSCE)* 2(1): 336-342.

APPENDIX

Simulation parameters of PMSG

Rs	1.9 Ω/phase
Ld	31 mH/phase
Lq	31 mH/phase
p	3
ψ_{pm}	1.1027 vs

CUK converter parameters

L_1	0.3 mH
L_2	0.5 mH
C_1	0.15 μF
C_2	0.16 mF

PI controller parameters

K_p	0.0005
K_i	0.003